

# Genome-wide DNA methylation profiling and its involved molecular pathways from one individual with thyroid malignant/benign tumor and hyperplasia

## A case report

Liang-Liang Cai, PhD<sup>a</sup>, Guo-Yan Liu, MD<sup>b</sup>, Chi-Meng Tzeng, PhD<sup>a,c,d,\*</sup>

### Abstract

**Background:** During development, methylation permanently changes gene activity, while aberrant gene methylation is key to human tumorigenesis. Gene methylation is an epigenetic event leading to gene silencing and some tumor suppressor genes that are aberrantly methylated in both thyroid cancer and benign thyroid tumor, suggesting a role for methylation in early thyroid tumorigenesis. Specific gene methylation occurs in certain types of thyroid cancer and depends on particular signaling pathways. Most reports rely on data from varied samples that vary tremendously with respect to methylation.

**Results:** We observed that hyperplastic/malignant (H/M) thyroid tissue and benign/malignant (B/M) tissue had the most profoundly methylated loci compared to hyperplastic/benign (H/B) tissue. These loci are mapped to 863 genes ( $|\Delta\beta \text{ value}| > 0.15$ ) in B/M and 1082 genes ( $|\Delta\beta \text{ value}| > 0.15$ ) in H/M. After bioinformatic analysis, these genes were found to be involved in T-cell receptor signaling pathway (B/M) and *Jak-Stat* signaling pathways (H/M).

**Conclusion:** Our study offers the most comprehensive DNA methylation data for thyroid disease to date, using 1 patient with 3 tissue types and high-resolution 450K arrays. Our data may lay the foundation for future identification of novel epigenetic targets or diagnosis of thyroid cancer.

**Abbreviations:** 1stExon = first exon sites, CTLA4 = cytotoxic T-lymphocyte antigen-4, DAG = diacylglycerol, GO = gene ontology, IP3 = inositol triphosphate, ISRE = IFN-stimulated response element, ITAMs = immunoreceptor tyrosine-based activation motifs, ITK = inducible T-cell kinase, KEGG = kyoto encyclopedia of genes and genomes, LAT = linker activator for T-cells, PTC = papillary thyroid cancer, TCR = T-cell receptor, TSS = transcription start site, UTR = untranslated regions.

**Keywords:** DNA methylation 450K array, thyroid benign, thyroid cancer, thyroid hyperplasia

Editor: László Géza Boros.

L-LC and G-YL contributed equally to this study.

**Authorship:** L-LC participated in the design of the study, performed experiments, and participated in the writing of the paper. G-YL participated in the design of the study and collected patients' samples. C-MT designed the study and participated in the writing of the paper.

**Funding:** This work was funded by The National Natural Science Foundation of China (grant number 81272445).

The authors have no conflicts of interest to disclose.

Supplemental Digital Content is available for this article.

<sup>a</sup> Translational Medicine Research Center, School of Pharmaceutical Sciences,

<sup>b</sup> Department of Gastrointestinal Surgery, Zhongshan Hospital, Xiamen University,

<sup>c</sup> Key Laboratory for Cancer T-Cell Theranostics and Clinical Translation,

<sup>d</sup> INNOVA Cell: TDX Clinics and TRANSLATE Health Group, Xiamen University, China.

\* Correspondence: Chi-Meng Tzeng, School of Pharmaceutical Sciences, Xiamen University, China (e-mail: cmtzeng@xmu.com).

Copyright © 2016 the Author(s). Published by Wolters Kluwer Health, Inc. All rights reserved.

This is an open access article distributed under the terms of the Creative Commons Attribution-Non Commercial License 4.0 (CCBY-NC), where it is permissible to download, share, remix, transform, and buildup the work provided it is properly cited. The work cannot be used commercially.

Medicine (2016) 95:35(e4695)

Received: 5 July 2016 / Received in final form: 2 August 2016 / Accepted: 2 August 2016

<http://dx.doi.org/10.1097/MD.0000000000004695>

## 1. Introduction

Thyroid cancer is the most common endocrine cancer—the most prevalent type of the papillary thyroid cancer (PTC)—and it is frequently diagnosed before adulthood. Deaths due to thyroid cancer have been low and stable for several years, compared with other cancers, but a clinically significant thyroid nodule may develop in 5% to 10% of the general population during their lifetime.<sup>[1]</sup>

Thyroid cancer is known as a multifactorial disease, which can be infected by susceptibility genes and environmental factors. There is a piece of evidence suggesting that interindividual differences in cancer susceptibility can also depend on epigenetic changes.<sup>[2]</sup> Epigenetics does not consider changes to underlying DNA sequences, but instead focuses on heritable changes in gene expression. DNA methylation is a type of epigenetic modification found in the human genome. Both tumor suppressor gene or DNA repair gene hypermethylation and repetitive DNA hypomethylation are closely related to different tumor types. Recently,<sup>[3]</sup> researchers confirmed that DNA methylation in a genome can be changed by DNA methyltransferase or by other factors such as histone modification, diet, environment, and RNA interference. With histone modification and chromatin remodeling, DNA methylation is important for transcriptional regulation.

Recently, epigenetic regulation of gene expression has emerged as a potentially important factor in tissue differences within a

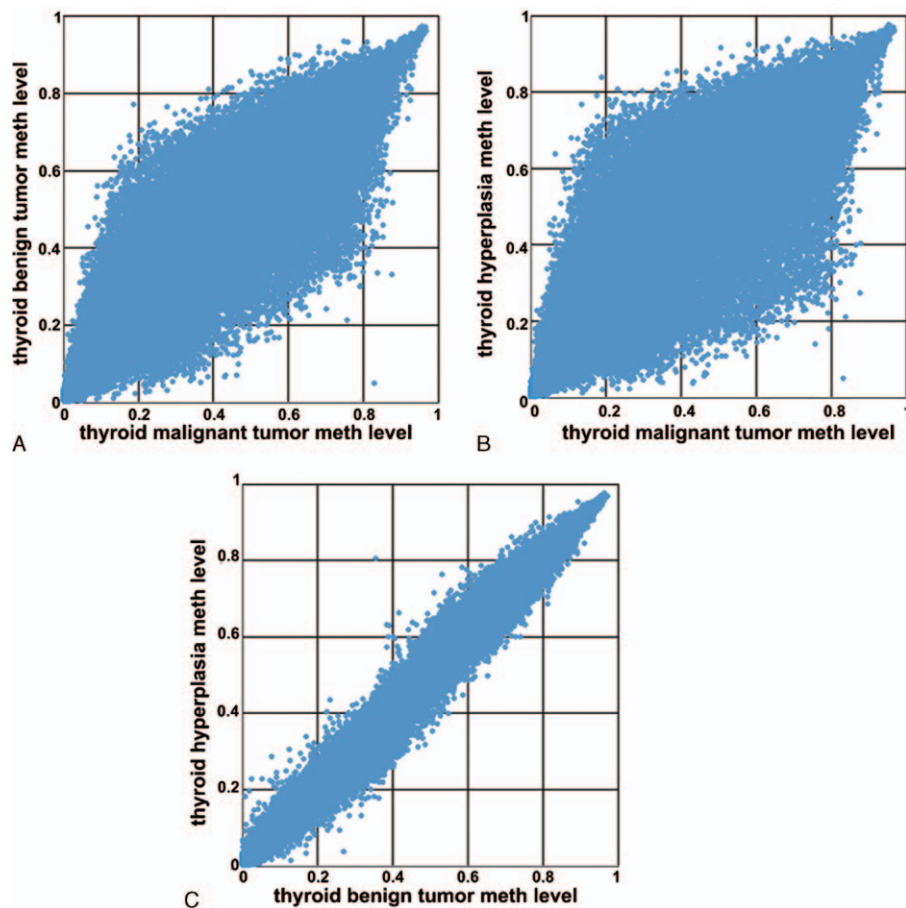


**Figure 1.** Comparisons of DNA methylation level in malignant, hyperplasia, and benign thyroid tissues.  $\beta$  value was used for estimation of methylation level using the ratio of intensities between methylated and unmethylated alleles, calculating by  $\beta$  value = methylated allele intensity (M)/(unmethylated allele intensity (U) + methylated allele intensity (M) + 100).  $\beta$  value reflects the methylation intensity at each CpG site.  $\beta$  value of 0 to 1 represented signifying percent methylation, from 0% to 100%, respectively, for each CpG site.

single disease. In chromosomal regions of tumor-associated genes, the epigenetic modifications can change important associated regulatory mechanisms for pathogenic malignant transformation. With DNA methylation, a methyl group is added to the fifth carbon on the cytosine residue in a CpG dinucleotide. CpG dinucleotides's rich regions (CpG islands) are usually located in the 5'-flanking gene promoter areas. Gene promoter methylation, particularly near the transcription start site, is associated with chromatin remodeling, which affects gene silencing.<sup>[4]</sup> DNA methylation is crucial for regulation gene expression and is known to be essential for the normal cellular development and maintaining tissue characters. Tumor suppressor gene inactivation by promoter hypermethylation is thought to be important in carcinogenesis. Thus, measuring DNA methylation in a genome-wide manner would be valuable for studying mechanisms of epigenetic control involved in gene expression regulation.

For personalized therapy, molecularly-defined tumor subgroup identification appears promising. For example, gene expression panels associated with breast cancer are now used clinically to provide individualized therapy. These panels, which depict carcinogen exposure-associated differences in individual tumors, include DNA hypermethylation involved in gene silencing as well as DNA hypomethylation, which is associated with oncogene activation and genomic instability.<sup>[5,6]</sup> DNA methylation pattern alterations in cancer-related gene promoter regions may be

associated with risk factors, clinical presentation, and thyroid cancer outcomes.

In this study, we use the Infinium Human Methylation 450 BeadChip platform to detect whole-genome methylation statistics of promoters and first exon sites (1st Exon) for thyroid cancerous, benign, and hyperplastic tissue. Data analysis includes a series of free-source software and package analyses of functional gene pathways. Also, significant biological functions and pathways related to these 3 tissue types are discussed. Our data should inform current opinions about gene methylation in thyroid tumorigenesis based on tissue epigenetics.

## 2. Materials and methods

### 2.1. Sample collection and DNA extraction

The patient thyroid samples were collected from the Zhongshan Hospital of Xiamen University. We obey the ethical standards of the Zhongshan Affiliated Hospital of Xiamen University committee when performing all procedures in this study involving human participants and with the 1964 Helsinki declaration and the comparable ethical standards or later amendments. The informed consent was obtained from all subjects. All experimental procedures were approved by the Zhongshan Affiliated Hospital of Xiamen University. Tissue was

**Table 1****The top 5 hyper- and hypo-methylation genes in thyroid malignant, benign, and hyperplasia tissue.**

Target ID	Delta_beta_value	UCSC_REFGENE_NAME	UCSC_REFGENE_GROUP	Approved name	Location
Thyroid benign and hyperplasia tissue					
cg02279953	-0.24362	SNORD114-11	TSS1500	Small nucleolar RNA, C/D box 114-11	14q32.31
cg02775223	-0.22987	DUXA	TSS1500	Double homeobox A	19q13.43
cg02467858	-0.18675	TTC23	TSS1500	Tetratricopeptide repeat domain 23	15q26.3
cg00461841	-0.14959	ATF7IP2	5'UTR	Activating transcription factor 7 interacting protein 2	16p13.2
cg04644523	-0.14951	LOC401387	1stExon	Homo sapiens hypothetical protein LOC401387	7q21.2
cg06806711	0.12517	MS4A1	1stExon	Membrane-spanning 4-domains, subfamily A, member 1	11q12-q13.1
cg00149213	0.13181	SLAMF1	TSS200	Signaling lymphocytic activation molecule family member 1	1q23.3
cg04754652	0.13994	GPR171	TSS200	G protein-coupled receptor 171	3q25.1
cg00240653	0.14061	KIAA0748	1stExon	Thymocyte expressed, positive selection associated 1	12q13.2
cg09852918	0.15568	CST7	TSS200	Cystatin F (leukocystatin)	20p11.21
Thyroid malignant and benign tissue					
cg00532474	-0.46566	PSTPIP2	TSS1500	Proline-serine-threonine phosphatase interacting protein 2	18q12
cg02192520	-0.44301	RDH5	1stExon	Retinol dehydrogenase 5 (11-cis/9-cis)	12q13-q14
cg01276497	-0.44262	C11orf91	TSS1500	Chromosome 11 open reading frame 91	11p13
cg04990202	-0.42484	S100A16	5'UTR	S100 calcium binding protein A16	1q21
cg00842076	-0.42407	FOXP3	5'UTR	Forkhead box N3	14q32.11
cg00041575	0.39712	TSPAN32	TSS1500	Tetraspanin 32	11p15
cg00569276	0.41124	PADI2	TSS1500	Peptidyl arginine deiminase, type II	1p35.2-p35.1
cg00231528	0.42581	PIK3CD	5'UTR	Phosphatidylinositol-4,5-bisphosphate 3-kinase, catalytic subunit delta	1p36.2
cg00903584	0.42853	PTPN7	5'UTR	Protein tyrosine phosphatase, nonreceptor type 7	1q32.1
cg00446123	0.50588	LIME1	TSS200	Lck interacting transmembrane adaptor 1	20q13.33
Thyroid malignant and hyperplasia tissue					
cg00028135	-0.506	ZBTB20	5'UTR	Zinc finger and BTB domain containing 20	3q13.2
cg02192520	-0.49738	RDH5	1stExon	Retinol dehydrogenase 5 (11-cis/9-cis)	12q13-q14
cg00142036	-0.49438	SEPHS1	5'UTR	Selenophosphate synthetase 1	10p14
cg00611789	-0.49393	CMYA5	TSS1500	Cardiomyopathy associated 5	5q14.1
cg01276497	-0.49311	C11orf91	TSS1500	Chromosome 11 open reading frame 91	11p13
cg00041401	0.48497	PTPN22	TSS200	Protein tyrosine phosphatase, nonreceptor type 22 (lymphoid)	1p13.2
cg00231528	0.48633	PIK3CD	5'UTR	Phosphatidylinositol-4,5-bisphosphate 3-kinase, catalytic subunit delta	1p36.2
cg00041575	0.49104	TSPAN32	TSS1500	Tetraspanin 32	11p15
cg00240653	0.50697	KIAA0748	1stExon	Thymocyte expressed, positive selection associated 1	12q13.2
cg00446123	0.63009	LIME1	TSS200	Lck interacting transmembrane adaptor 1	20q13.33

divided into 3 subtypes: papillary thyroid cancer, benign tissue, and hyperplastic tissue and stored at  $-80^{\circ}\text{C}$ . DNA from each tissue was extracted with a QIAamp DNA Mini Kit (QIAGEN) according to the manufacturer's instructions and stored at  $-80^{\circ}\text{C}$  to prevent degradation. Formalin-fixed, paraffin-embedded specimens were microscopically examined using H&E staining and reviewed by a pathologist (see in Supplement File, <http://links.lww.com/MD/B221>).

## 2.2. Methylation chip experiment

This Infinium Human Methylation 450 BeadChip Kit can be used to acquire >450,000 methylation site. These sites cover 99% of RefSeq genes. These methylated region distributed across the whole body of gene, including its TSS, 5'-untranslated regions (UTR), 3'-UTR, first exon, and gene body. In this study, we filtered the transcription start site (TSS) and first exon sites (1st Exon), which have most significant influence on the gene.

According to the standard protocol, the microarray hybridization and scanning data were collected. After bisulfite treatment, the whole genome from each tissue was amplified, enzymatically fragmented and hybridized to the Illumina Infinium HumanMethylation450 BeadChip kits. Following

hybridization, allele specific single-base extension and staining were performed. Then, the BeadChips were imaged on Illumina BeadArray Reader platform. The Illumina's BeadScan software was used for extracting the image intensities. The fluorescent signals from methylated and unmethylated alleles represented methylation data point from which the background intensity was then subtracted. Applying the default settings, DNA methylation data were processed using the GenomeStudio software (Illumina). For array data points, both methylated (Cy5) and unmethylated (Cy3) alleles were used to create the average methylation ( $\beta$ ) value after 30 replicate methylation data collection. In addition, we excluded the methylation data on X chromosome from the analysis. The filtered methylation sites were then mapped to its potential regulated gene defined in the UCSC Genome Browser HG19 RefSeq database.

## 2.3. Chip data analysis

We analyzed methylation data using the free and open-resources software R, which contains a suite of packages for data handling, such as ggplots2<sup>[7]</sup> (a powerful data visualization tool), clusterProfiler<sup>[8]</sup> (for analyzing and visualizing functional profiles-gene ontology (GO) and kyoto encyclopedia of genes

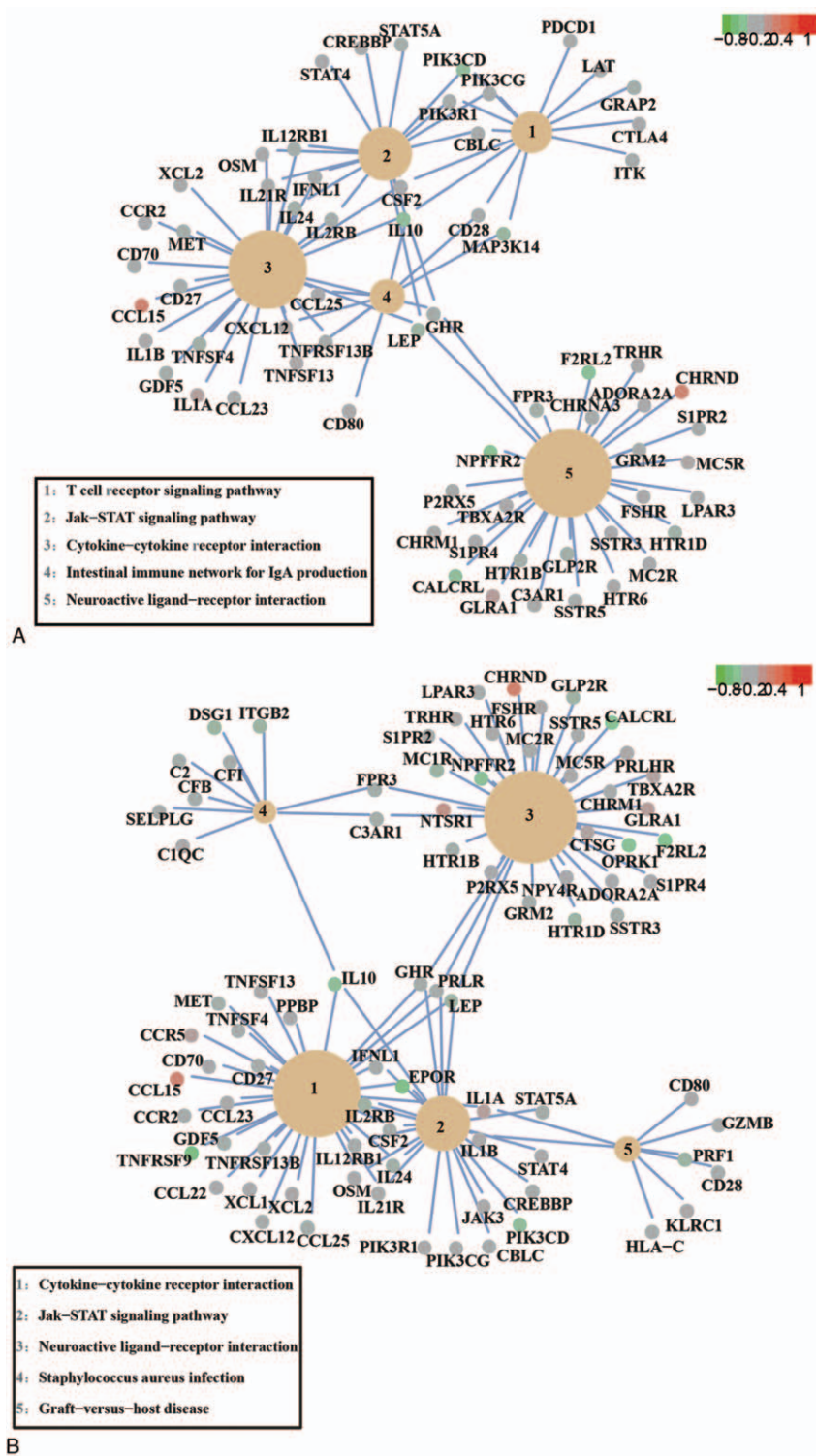


**Figure 2.** Category Net Plot of KEGG enrichment. The top 5 (most significant) categories of each cluster (A: benign and malignant; B: hyperplastic and malignant) was plotted: dot sizes were based on their corresponding row “percentage” as a default parameter to represent dot size. Some categories may contain many genes, so dots for those categories are too small to compare. Dots in the plot are colored based on their  $\Delta\beta$  value. Color gradient ranging from green to red corresponds to order of increasing  $\Delta\beta$  value.  $\Delta\beta$  value displayed differential methylation levels of malignant compared with benign in A (malignant compared with hyperplastic in B). Green = hypomethylation, KEGG = kyoto encyclopedia of genes and genomes, red = hypermethylation.

and genomes (KEGG)-of genes and gene clusters). After clustering analysis, we identified common themes of particular gene clusters and compared biological themes among gene clusters. To bridge this gap, we choose clusterProfiler, for

comparing and visualizing functional roles among gene clusters. All software parameters analyzed are shown in R script (See in Supplement File, <http://links.lww.com/MD/B221>).

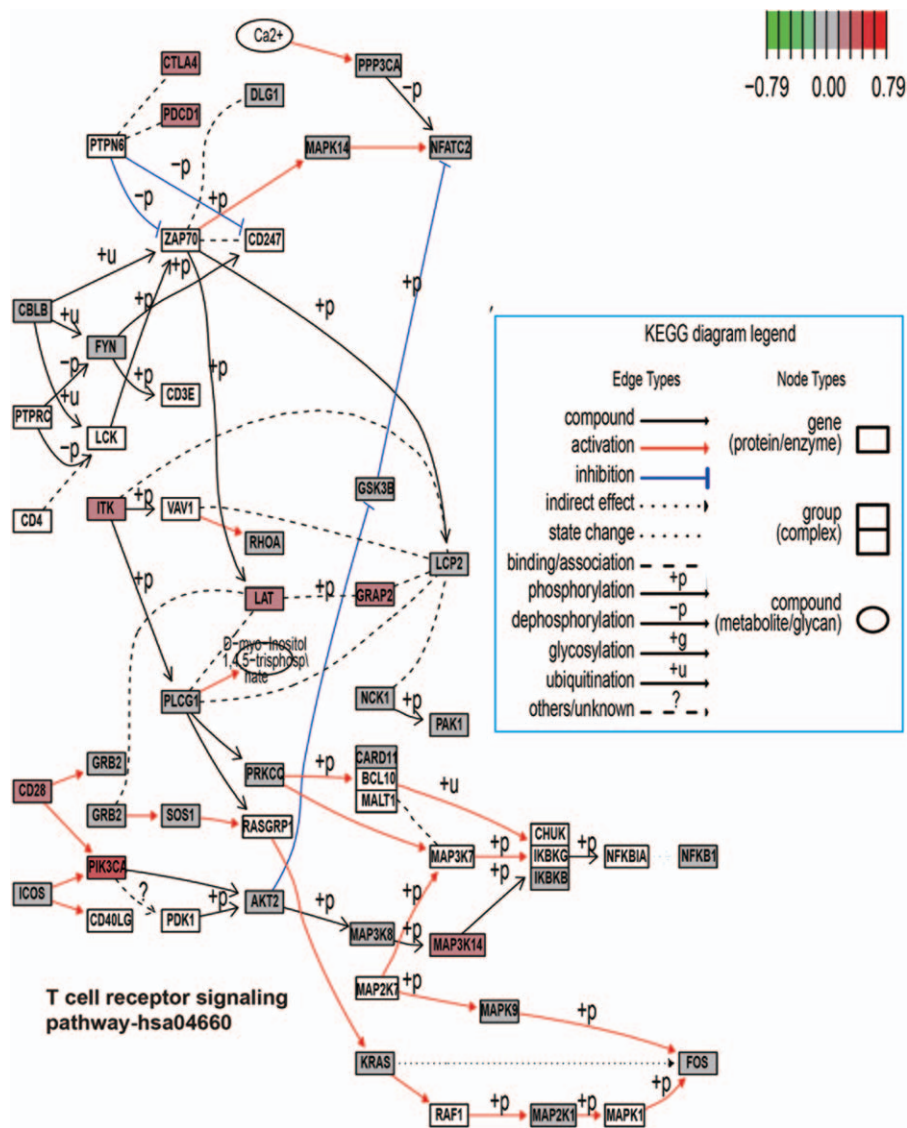


**Figure 3.** KEGG in Graphviz view of T-cell receptor signaling pathways on a canonical signaling pathway with gene methylation chip data. The methylation chip data were integrated, analyzed, and visualized in the T-cell receptor signaling pathways. Color gradient ranging from green to red corresponds to order of increasing  $\Delta\beta$  value.  $\Delta\beta$  value displayed differential methylation levels of malignant compared with benign. Green = hypomethylation, KEGG = kyoto encyclopedia of genes and genomes, red = hypermethylation.

### 3. Results and discussion

#### 3.1. Chip data analysis across 3 types of thyroid tissue

In this study, we visualized these methylation data using the matrix chart (Fig. 1), which directly describes methylation at the whole genome level. Significant differences in gene methylation can be used to describe tissue differences  $\Delta\beta$  values (difference among 3 samples) can be obtained and ranked (showing in Table 1) to show the top 5/5 hyper/hypomethylation genes among H/M, B/M, and B/M and this can be used ( $|\Delta\beta \text{ value}| > 0.15$ ) for bioinformatics analysis. Then, the methylation loci are mapped to 863 genes ( $|\Delta\beta \text{ value}| > 0.15$ ) in B/M and 1082 genes ( $|\Delta\beta \text{ value}| > 0.15$ ) in H/M. To understand hyper/hypomethylation of genes interaction with physiological processes, a biochemical (based R) package, clusterProfiler<sup>[8]</sup> was used for pathway analysis of KEGG (see Figs. 2–4). Data depict differences in gene

methylation among hyperplastic, benign and malignant thyroid tissue involved in T-cell receptor signaling pathway (B/M), *Jak-Stat* signaling pathways (H/M).

#### 3.2. T-cell receptor signaling pathway involved in benign and malignant thyroid tumor

The gene methylation status of B/M in the T-cell receptor signaling pathway is depicted in Figs. 2A and 3 Figs. 2 and 3. In the immune response, T-cell receptor (TCR) stimulation can induce a series of intracellular signaling cascades and these cascades regulate a series of important functions, such as T-cell development, homeostasis, activation, acquisition of effector functions, and apoptosis. CD3 molecules complexing with the TCR heterodimer form immunoreceptor tyrosine-based activation motifs (ITAMs), which are important for signal transduction

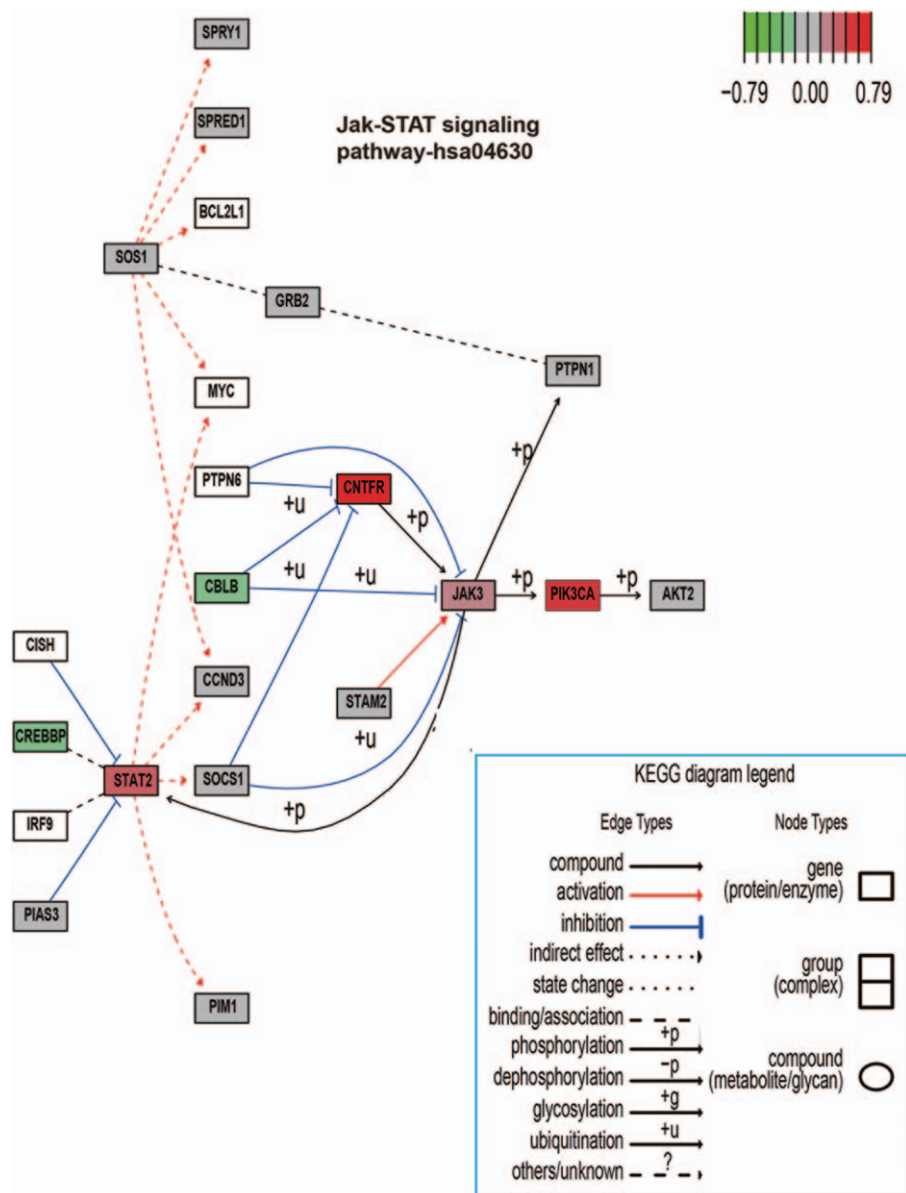


**Figure 4.** KEGG in Graphviz view of Jak-STAT signaling pathways on a canonical signaling pathway with gene methylation chip data. The methylation chip data were integrated, analyzed, and visualized in the Jak-STAT signaling pathways. Color gradient ranging from green to red corresponds to order of increasing  $\Delta\beta$  value.  $\Delta\beta$  value displayed differential methylation levels of malignant compared with hyperplastic. Green=hypomethylation, KEGG=kyoto encyclopedia of genes and genomes, red=hypermethylation.

in immune cells. ITAMs orchestrate sequential activation of transmembrane adaptors: linker activator for T-cells (LAT), which ultimately induce effector functions.<sup>[9-11]</sup> During T-cell activation, the CD28 molecule provides an essential costimulatory signal. This signal increases the IL-2 production, T-cell proliferation, and protects cell from increasing the immune response and preventing cell death. After being activated by the CD28 molecule, Lck subsequently stimulates and activates the tyrosine kinases: Fyn and ZAP70. ZAP70 remains associated with TCR and induces activation of LAT, which binds to the adaptor growth factor receptor-IL-2 inducible T-cell kinase (ITK). Besides this, LAT stimulates 1 critical protein phospholipase-C- $\gamma$ 1 that plays an important role for the production of the

second messengers diacylglycerol (DAG) and inositol triphosphate (IP<sub>3</sub>).<sup>[12-15]</sup> The activated LAT interacts with GRB2, by this manner GRB2 and GRAP-associated SOS are pooled to the cell membrane and then potentially activate Ras.<sup>[14]</sup> The activated Ras will lead to the activation of serine/threonine kinases: Raf1, MAPK/ERK kinase.<sup>[9,14-16]</sup> In this pathway, cytotoxic T-lymphocyte antigen-4 (CTLA4), which serves as a natural inhibitor, negatively regulates T-cell activation, so that once T-cells become activated by the disease that turns them on and the body can naturally decrease T-cell pathways to control activity. CTLA4 can interact with SHP2 and inhibits TCR phosphorylation. When control of TCR signaling is needed, ZAP70 recruits CTLA4 to the membrane.<sup>[17,18]</sup>

### 3.3. *Jak-Stat* signaling pathway involved in hyperplasia and malignant thyroid diseases

In development, cellular differentiation and homeostasis, *Jak-Stat* signaling pathways mediates essential cell-to-cell information transduction. Thus, dysregulation of this pathway has been associated with human malignancies. We created a view of this pathway involving the methylation status of H/M tissue in Figs. 2B and 4 Figs. 2 and 4. *Jak3* was a member of nonreceptor protein tyrosine kinases family. *Stat2*, which is encoded by distinct genes, is a Signal transducer and activator. The *Jak-Stat* signaling pathway is regulated by diverse intrinsic and environmental stimuli, which increase cell/tissue response plasticity.<sup>[19,20]</sup> The phosphorylated *stat2* dimerize complexed with IRF9/ISGF3G enters into the nucleus as transcription factor. The interferon-stimulated genes's transcription was activated by the binding of ISGF3 and IFN-stimulated response element (ISRE).<sup>[21,22]</sup> In an indirect manner, the *Jak/Stat* signaling pathway also promotes *Ras* signaling via *Socs*' transcriptional activation. The activated *Socs* binds *RasGAP*, which plays a role of negative regulator of *Ras* signaling, and then reduces *Ras*'s activity. Reciprocally, *Rtk* signaling pathway's activity promotes the *Jak/Stat* signaling by first activating some RTKs and next allowing *Rtk/Ras* pathway stimulation to active the downstream *MAPK*.

### 4. Conclusions

In our study, nonessential data (or "noise") from inter-individual samples based on age, gender, and ethnicity (among others) were excluded and we offer a more precise profile for methylation differences among 3 types tissue (hyperplasia, benign, and malignant). Data indicate that hyperplastic/ malignant groups and benign/malignant groups were the most different and hyperplastic and benign tissues differed only slightly.

The T-cell receptor signaling pathway may play its role in benign and malignant thyroid tumor. An immune response involves T-cell activation, defends against tumor cells, and participates in rejection reactions. T-cell receptor stimulation may provoke proliferation, lack of a response to future stimuli, or cell death such as thymocytes. Because T-cells have so many roles in the immune response, it is important to understand what should assist us to comprehend how immune regulation dysfunction causes immune diseases and how immune system can be used for overcoming thyroid diseases.<sup>[23,24]</sup>

The *Jak-Stat* signaling pathway may involved in hyperplasia and malignant thyroid diseases. Our study shows that *STATs* were involved not only in breast cancer, myeloma, and head and neck cancer<sup>[25,26]</sup> but also thyroid tumor diseases by the hypermethylation and hypometylation of key genes.

However, structural epigenetic changes in DNA methylation do not necessarily result in alterations in gene expression, which is functionally more important than DNA methylation. Synergistic analysis of DNA methylation and gene expression may maximize the opportunity to insight upon the pathogenesis of thyroid cancer. Thus, more research is needed to extend our data

suggesting that compared to benign and hyperplastic thyroid tissue, malignant thyroid tissue is the most methylated, and that methylation is important for cancer initiation.

### References

- [1] Mazzaferri EL. Management of a solitary thyroid nodule. *N Engl J Med* 1993;328:553–9.
- [2] Dawson MA, Kouzarides T. Cancer epigenetics: from mechanism to therapy. *Cell* 2012;150:12–27.
- [3] Zhang LL, Wu JX. DNA methylation: an epigenetic mechanism for tumorigenesis. *Yi Chuan* 2006;28:880–5.
- [4] Bird A. DNA methylation patterns and epigenetic memory. *Genes Dev* 2002;16:6–21.
- [5] Baylin SB, Ohm JE. Epigenetic gene silencing in cancer—a mechanism for early oncogenic pathway addiction? *Nat Rev Cancer* 2006;6:107–16.
- [6] Jones PA, Baylin SB. The fundamental role of epigenetic events in cancer. *Nat Rev Genet* 2002;3:415–28.
- [7] Wickham H. ggplot2: elegant graphics for data analysis. 2009; New York:Springer, (978-0-387-98140-6).
- [8] Yu G, Wang LG, Han Y, et al. clusterProfiler: an R package for comparing biological themes among gene clusters. *OMICS* 2012;16:284–7.
- [9] Davis MM. A new trigger for T cells. *Cell* 2002;110:285–7.
- [10] Okkenhaug K, Vanhaesebroeck B. PI3K in lymphocyte development, differentiation and activation. *Nat Rev Immunol* 2003;3:317–30.
- [11] Coombs D, Kalergis AM, Nathenson SG, et al. Activated TCRs remain marked for internalization after dissociation from pMHC. *Nat Immunol* 2002;3:926–31.
- [12] Lin J, Weiss A. T cell receptor signalling. *J Cell Sci* 2001;114(pt 2):243–4.
- [13] Okkenhaug K, Bilancio A, Emery JL, et al. Phosphoinositide 3-kinase in T cell activation and survival. *Biochem Soc Transact* 2004;32(pt 2):332–5.
- [14] Gong Q, Cheng AM, Akk AM, et al. Disruption of T cell signaling networks and development by Grb2 haploid insufficiency. *Nat Immunol* 2001;2:29–36.
- [15] Davidson D, Bakinowski M, Thomas ML, et al. Phosphorylation-dependent regulation of T-cell activation by PAG/Cbp, a lipid raft-associated transmembrane adaptor. *Mol Cell Biol* 2003;23:2017–28.
- [16] Alonso A, Rahmouni S, Williams S, et al. Tyrosine phosphorylation of VHR phosphatase by ZAP-70. *Nat Immunol* 2003;4:44–8.
- [17] Gough SC, Walker LS, Sansom DM. CTLA4 gene polymorphism and autoimmunity. *Immunol Rev* 2005;204:102–15.
- [18] Lin H, Rathmell JC, Gray GS, et al. Cytotoxic T lymphocyte antigen 4 (CTLA4) blockade accelerates the acute rejection of cardiac allografts in CD28-deficient mice: CTLA4 can function independently of CD28. *J Exp Med* 1998;188:199–204.
- [19] Ananthakrishnan R, Hallam K, Li Q, et al. JAK-STAT pathway in cardiac ischemic stress. *Vasc Pharmacol* 2005;43:353–6.
- [20] Walker JG, Smith MD. The Jak-STAT pathway in rheumatoid arthritis. *J Rheumatol* 2005;32:1650–3.
- [21] Marrero MB. Introduction to JAK/STAT signaling and the vasculature. *Vasc Pharmacol* 2005;43:307–9.
- [22] Gao B. Cytokines, STATs and liver disease. *Cell Mol Immunol* 2005;2:92–100.
- [23] Anderton SM. Avoiding autoimmune disease—T cells know their limits. *Trends Immunol* 2006;27:208–14.
- [24] Waldmann TA. Effective cancer therapy through immunomodulation. *Ann Rev Med* 2006;57:65–81.
- [25] Poehlmann TG, Busch S, Mussil B, et al. The possible role of the Jak/STAT pathway in lymphocytes at the fetomaternal interface. *Chem Immunol Allergy* 2005;89:26–35.
- [26] Grote K, Luchtefeld M, Schieffer B. JANUS under stress—role of JAK/STAT signaling pathway in vascular diseases. *Vasc Pharmacol* 2005;43:357–63.